




Sensory and memory processing in old female and male Wistar rat brain, and its relationship with the cortical and hippocampal redox state

Roberto Santín-Márquez · Belén Ramírez-Cordero · Rafael Toledo-Pérez · Armando Luna-López · Norma E. López-Diazguerrero · Ulalume Hernández-Arciga · Marcel Pérez-Morales · Juan José Ortiz-Retana · Martín García-Servín · Sarael Alcauter · Braulio Hernández-Godínez · Alejandra Ibañez-Contreras · Luis Concha · Beatriz Gómez-González · Mina Königsberg 

Received: 4 October 2020 / Accepted: 9 March 2021

© American Aging Association 2021

Abstract The brain is one of the most sensitive organs damaged during aging due to its susceptibility to the aging-related oxidative stress. Hence, in this study, the sensory nerve pathway integrity and the memory were evaluated and related to the redox state, the antioxidant enzymes function, and the protein oxidative damage in the brain cortex (Cx) and the hippocampus (Hc) of young (4-month-old) and old (24-month-old) male and female Wistar rats. Evoked potentials (EP) were performed for the auditory, visual, and somatosensory pathways. In both males and females, the old rat groups' latencies were larger in almost all waves when compared to the young same-sex animals. The novel object test was performed to evaluate memory. The superoxide

dismutase and catalase antioxidant activity, as well as the protein oxidative damage, and the redox state were evaluated. Magnetic resonance (MR) imaging was used to obtain the diffusion tensor imaging, and the brain volume, while MR spectroscopy was used to obtain the brain metabolite concentrations (glutamine, glutamate, Myo-inositol, N-acetyl-aspartate, creatine) in the Cx and the Hc of young and old females. Our data suggest that, although there are limited variations regarding memory and nerve conduction velocity by sex, the differences concerning the redox status might be important to explain the dissimilar reactions during brain aging between males and females. Moreover, the increment in Myo-inositol levels in the Hc of old rats

R. Santín-Márquez · B. Ramírez-Cordero · R. Toledo-Pérez · N. E. López-Diazguerrero · U. Hernández-Arciga · M. Königsberg (✉)
Departamento de Ciencias de la Salud, DCBS, Universidad Autónoma Metropolitana Iztapalapa, México, CDMX 09340, México
e-mail: mkf@xanum.uam.mx

A. Luna-López
Instituto Nacional de Geriátria, SSA, CDMX 10200, México

M. Pérez-Morales · B. Gómez-González
Departamento de Biología de la Reproducción, DCBS, Universidad Autónoma Metropolitana Iztapalapa, México, CDMX 09340, México

J. J. Ortiz-Retana · S. Alcauter · L. Concha
Laboratorio Nacional Enfocado en Imagenología por Resonancia Magnética, Instituto de Neurobiología, UNAM, Juriquilla, Mexico

M. García-Servín
Bioterio, Instituto de Neurobiología, UNAM, Juriquilla, Mexico

B. Hernández-Godínez · A. Ibañez-Contreras
APREXBIO S.A.S de C.V., Laboratorio de Primatología, CDMX, México

R. Santín-Márquez · R. Toledo-Pérez
Posgrado en Biología Experimental, UAMI, México, México

and the brain volume decrease suggest that redox state alterations might be correlated to neuroinflammation during brain aging.

Keywords Evoked potentials, · Memory, · Oxidative stress, · Magnetic resonance, · Brain, · Aging, · Sexual dimorphism

Introduction

Aging is currently considered a multifactorial, universal, progressive, and deleterious process that occurs with time and results in a decline in the organism's physiological functions, increasing its vulnerability to illness and death [1, 2]. Human life expectancy has increased in recent decades, and it is known that women live longer than men. Moreover, they survive better in adverse situations [3]. The fact that females and males age differently is supported by numerous reports where genetic manipulations or pharmacological interventions favored one or the other sex [4, 5]. This pattern is apparently conserved in several mammalian species (but not in all). It has been mainly explained due to the presence of sex hormones, such as estrogen [6], and, more recently, by the hormonal interplay of the whole hypothalamic–pituitary–gonadal axis [5]. Still, other factors may also be involved, not only in promoting longevity, but also in increasing the healthspan.

It is known that the nervous system is one of the most affected systems during aging, and that men and women have different propensities to present neurodegenerative diseases. Yet, for many years, female studies have been under-represented in neuroscience, since only male animals are typically used to perform the experiments [7]. In recent years, it is increasingly common to find reports of sex differences in neurobiology and behavior. However, most of those studies are performed in young individuals, so, normal age-related changes are usually not evaluated. Moreover, the majority of them also focus on the differences orchestrated directly by sex hormones [8].

The brain's intrinsic characteristics make it especially susceptible to changes in the redox state. Some examples of these characteristics are its high oxygen consumption that results in considerable reactive oxygen species (ROS) generation, its high lipid content, the auto oxidation of neurotransmitter precursors, its low antioxidant capacity, and its high iron content compared to other organs [9]. Therefore, many of the physiological

changes that promote mental and motor deterioration during normal aging, as well as neurodegenerative diseases, have been associated to oxidative stress. Alterations in the redox state disturb processes such as sensory pathway integration, nerve conduction velocity, memory, circadian rhythm, and others [10–12]. Therefore, in this study, we wanted to analyze sex differences in the brain functionality and in the cognitive decline during normal aging, and to relate them with changes in the redox state. Recently, sex differences in the brain redox state were shown during aging [13]. Although, it has been established that oxidative stress might not be the principal cause of aging [14], alterations in the redox state are known to play important roles in the central nervous system (CNS) functional decline and degeneration [15]; so, besides the hormonal changes, modifications in the redox state might account for the different responses observed in males and females. Hence, to better understand the sex differences in the brain functional decline during normal aging, biochemical assays to evaluate oxidative stress were run along with the non-invasive functional tests using female and male Wistar rats aged 4 and 24 months. The superoxide dismutase [16] and the catalase (CAT) antioxidant activity, as well as the protein oxidative damage, and the redox state (the reduced and oxidized glutathione ratio, GSH/GSSG), were evaluated. Changes in the sensory pathways function through evoked potentials (EP) were quantified to evaluate a probable decrease in the conduction velocity due to myelin loss or degeneration. The novel object recognition test was also used to evaluate the recognition memory, which is dependent on the sensory inputs and a brain circuit conformed by the hippocampus, and the frontal and rhinal cortices [17].

Another series of experiments were performed only in young and old females; diffusion tensor imaging (DTI) was used as the indicator of nerve fiber integrity and myelination [18–20], along with anatomical and metabolic determinations that were also non-invasively obtained through magnetic resonance imaging (MRI) and spectroscopy (MRS), since brain metabolite alterations during aging have been related to cognitive decline [21]. The brain cortex (Cx), the hippocampus (Hc), and the total brain volume were measured and MRS was used to quantify the molecular concentrations of glutamine, glutamate, Myo-inositol, N-acetyl aspartate, glycerophosphocholine, and creatine.

Our data suggest that, although there are limited variations regarding the memory and nerve conduction

velocity by sex, the differences concerning the redox status might be important to explain the dissimilar reactions during brain aging between males and females.

Material and methods

Chemicals

All chemicals and reagents were purchased from Sigma Chemical Co. (St. Louis, MO). The reagents obtained from other sources are detailed throughout the text.

Animals

The Wistar rats (*Rattus norvegicus*) were provided by the closed breeding colony at the Universidad Autónoma Metropolitana-Iztapalapa (UAM-I). Young (4-months old) and old (24-months old) animals were housed five-per-cage in polycarbonate cages in a 12-h light-dark cycle and provided with a standard commercial rat diet (Harlan 2018S, USA), and water ad libitum. The animals' health status was constantly evaluated. An acceptable state of health was considered when the animals did not have tumors, nor skin or ear infections, and when they ate and drank properly. Rats with tumors and those that went blind were discarded from the study. All animals' procedures were strictly carried out according to the Mexican Official Ethics Standard NOM-062-ZOO-1999, and the Standard for the disposal of biological waste (NOM-087-ECOL-1995). The rats were euthanized by decapitation, according to the NOM-062-ZOO-1999, section 9.5.3.3. The protocol was also approved by the Internal Committee of Laboratory Animals Care and Use, as well as the Ethics and Research Commissions of APREXBIO S.A.S. de C.V.

Biochemical assays

The Cx and the Hc were dissected and stored in a -70°C ultra-freezer for the biochemical assays.

Protein extraction

One hundred milligrams from each dissected tissue was taken and mechanically homogenized. Lysis buffer (DTT 10 mM, Phenylmethylsulfonyl fluoride (PMSF) 10 mM, 1 Roche completeTM Mini tablet, 10 mL T-PER) was added to the homogenate and the mixture was

centrifuged at 13,500 rpm at 4°C for 15 min. The supernatants were separated and stored in a -70°C ultra-freezer. Before each assay, the protein concentration was determined by spectrophotometry at 595nm, using a commercial Bradford reagent (Bio-Rad, Hercules, CA, USA).

SOD antioxidant activity

The antioxidant enzyme activity was analyzed by spectrophotometry (Thermo ScientificTM GENESYS 10S UV-Vis; Madison, WI USA) through the xanthine/xanthine oxidase system based on Paoletti, *et al* [22] protocols modified by [23]. Twenty five microliters of the sample plus 25 μL of xanthine oxidase solution freshly prepared (0.1 U of XO dissolved in 1 mL of 2 M ammonium sulfate) were used, and were added to 1.45 ml of the working solution (10 μM xanthine, nitro blue tetrazolium (NBT) 250 μM and EDTA 10 μM dissolved in a sodium carbonate buffer solution 50mM). The xanthine/xanthine oxidase system continuously produces superoxide anion, which reacts with the NBT and generates a formazan salt as a product that was measured at 560nm every 30 s along 5 min spectrophotometrically. One unit of enzyme is considered as the amount of SOD needed to inhibit 50% of the superoxide reaction with the NBT.

Catalase antioxidant activity

The antioxidant enzyme activity was analyzed by spectrophotometry (Thermo ScientificTM GENESYS 10S UV-Vis; Madison, WI USA) through the Aebi protocol [24] modified by [25], evaluating the decline in H_2O_2 levels at 240 nm every 15 s along 3 min. One catalase unit was considered as the amount of enzyme necessary to catalyze 1 μmol of H_2O_2 per min.

Protein oxidative damage

The carbonyl concentration was determined as reported elsewhere [23]. Each protein sample was centrifuged at 13,500 rpm at 4°C for 15 min. The supernatants were separated in 1.5-mL tubes and 20 μL were taken and added into 96 wells plates with 20 μL of DNPH 10 mM in 0.5 M H_3PO_4 (DNPH final concentration 4 mM). The samples were incubated for 10 min in the dark with constant agitation. Afterwards, NaOH 1.2M was added

and incubated in the dark for 10 min at room temperature (50 μL was the total volume in each well). The absorbance was determined at 450 nm against a blank where an equal volume of buffer solution substituted the protein solution. The carbonyl content was calculated as $(\text{Abs}_{450}/E)/\text{total protein content of the sample}$, where E = extinction factor of 46.1.

GSH/GSSG determination

The GSH/GSSG quotient was determined by high-performance liquid chromatography (HPLC) [26]. The brain cortex (100 mg) and the hippocampus (50 mg) were homogenized mechanically in 1 mL of perchloric acid/BPDS 1 mM. Then, the homogenate was centrifuged at 13,500 rpm at 4°C for 5 min. The supernatants were separated and diluted with PBS (1:10 v/v). Each sample (50 μL) was injected on a binary pump (Waters 1525) coupled to a UV/visible detector (Waters 2489) at 210 nm. The stationary phase was performed in a 4.6×250 mm Eclipse XDB-C18 column, and a 5- μm particle size using KH_2PO_4 20mM and 1% pH 2.7 acetonitrile as mobile phase with a 1mL/min flux. The area under the curve was determined through a standard curve using 10, 25, 50, 100, 200, and 400 μM GSH and GSSG concentrations.

Neurophysiological assays

The evoked potentials were performed in the APREXBIO's Neurophysiology Laboratory and recorded in a NEURONICA 5® equipment (Neuronic®, La Habana, Cuba) using subcutaneous needle electrodes (Ambu®, Spain) located according to the 10/20 International System. The electrophysiological assays were registered employing $<5\Omega$ impedances. Chemical sedation by intramuscular administration was required for the application of the electrophysiological tests, using an anesthetic cocktail, which contained ketamine (100 mg/kg; Anesket® Pisa Farmacéutica Mexicana) and xylazine (5 mg/kg; Procin® Pisa Farmacéutica Mexicana).

Brainstem auditory evoked potentials (BAEP)

The ear stimulation was evaluated with “clicks” or clicking rarefaction (negative polarity) at a 50-dB intensity, with a 0.1-ms duration [12]. The “clicks” came out through headphones that were part of the equipment.

The contralateral ear was masked with white noise at 20 dB below the intensity explored. The electrode impedance was maintained below 5 k Ω . In order to obtain the electrical activity recording, the stimulation with 50 dB started at the left ear and then continued to the right one. The negative electrodes were located on the A1 or A2 brain derivation on the ipsilateral side of the stimulated ear, and the positive electrode was located on Fz, the ground electrode was located on the base of the tail. The bandpass filter was set up between 100 to 3000 Hz with 10 μV sensitivity, and an average of 2000 stimuli was administrated.

Visual evoked potentials (VEP)

The negative electrode was located on the occipital zone [12] and the positive electrode was located on Fz, the ground electrode was located on the base of the tail. The bandpass filter was set up between 1 to 100 Hz with 50 μV sensitivity, and an average of 50 stimuli of 200 ms was administered. Both eyes were stimulated by luminous flashes.

Medial nerve somatosensory evoked potentials (MSSEP) and tibial nerve somatosensory evoked potentials (TSSEP)

For the MSSEP recording, the negative electrodes were located on the 7th cervical disk (C7) and the contralateral somatosensory cortex (C3' or C4'), and the positive electrode was located on the frontal zone (Fz). For the TSSEP recording, the negative electrodes were located on the 4th lumbar disk (L4) and the contralateral somatosensory cortex (C3' or C4'), and the positive electrode was located on Fz. In both cases, the ground electrode was located on the base of the tail.

Standard somatosensory evoked potentials were obtained by 100 μs square monophasic electric pulses with an intensity of 2 mA, the stimulation frequency was of 1.1 stimuli/s, with an average of 250 stimuli administrated. The bandpass filter was set up between 3 to 3000 Hz.

Novel object recognition test (NOR)

The NOR test has been used to evaluate the short-term and working memory, as well as their decay during aging in Wistar rats [27]. Here, the NOR test was performed using a $45 \times 45 \times 45$ -cm acrylic observation

box; each rat was introduced into the observation box for 5 min a day for 3 days, as a training period. On the fourth day, a pre-test was performed. Two random objects, with different geometric shapes, were placed in the box and the animals were allowed to explore for 5 min both objects. The exploration time for each object was recorded. The objects were changed for each rat. On the fifth day, the actual test was performed by placing just one of the objects previously presented to the animal along with a novel object. The animals were then allowed to explore again for 5 min. The exploration time was recorded, as well as the interaction-time and the interaction-number spent with the old and new objects. The Preference index was calculated dividing the time spent exploring the novel object by the total exploration time multiplied by 100, in order to obtain a percentage value.

Magnetic resonance imaging (MRI)

All the imaging experiments were performed at the National Laboratory for Magnetic Resonance Imaging, using a 7 T Bruker PharmaScan 70/16 scanner (Ettlingen, Germany), with a 2x2 array surface RF coil. Four and 24-month-old female rats were used. All specimens were anesthetized with isoflurane in an air mixture using 3.5 % for induction, then maintained in 0.8–1.5% isoflurane during the MRI scanning. The respiration rate was continually monitored. The body temperature was maintained at 37 °C by warm water circulation underneath the animal. High-resolution anatomical images were acquired in axial, coronal, and sagittal views to determine the specimen's correct position. T2-weighted MR imaging was performed using rapid acquisition with refocused echoes sequence with the following parameters: TR = 2500 ms, TE = 33 ms, number of echoes = 8, averages=3, field of view = 35 · 35 mm², matrix = 256 · 256, resulting resolution: 0.137 · 0.137 mm², slice thickness = 0.5 mm and acquisition time = 4 min. The MRI scans were exported to DICOM format using Paravision 6.01 and analyzed using ImageJ [28]. The regions of interest (ROIs), i.e., the brain cortex (Cx) and the hippocampus (Hc), were defined in coronal sections by RSM & BRC. For the Cx, within the slice in bregma -2.0 mm with approximately 100 voxels covering the primary somatosensory region and for the Hc, within the slice in bregma -2.7 mm with at least 60 voxels covering the CA1 region.

Diffusion tensor imaging (DTI)

DTI data were acquired using a spin-echo EPI sequence with the parameters: TR = 2250 ms, TE = 31.32 ms, flip angle = 90°, averages = 4, field of view = 20 × 14 mm², matrix = 150 × 104 pixels, resolution = 0.133 × 0.135 mm², slice thickness = 0.75 mm, number of acquisitions = 1. The diffusion weighting was isotropically distributed along 40 directions with *b* values = 650 and 2000 s/mm². Additionally, six images with no diffusion weighting were acquired (*b* value = 0 s/mm²). The DTI data acquisition took 13 min. The pre-processing and analysis of diffusion weighted-images were performed using the MRtrix3 and FSL software (version 5.0.6; FMRIB, Oxford, UK) [29]. Each scan was visually inspected for quality. The diffusion weighted images were denoised and then corrected for eddy current distortions and head movement using eddy correction (FSL's tool). The measured water diffusion was fitted to a tensor model with a 3 × 3 symmetrical matrix with eigenvalues λ_1 , λ_2 , and λ_3 , and its corresponding eigenvectors ν_1 , ν_2 , and ν_3 . The eigenvalue λ_1 is related to the diffusivity along the principal axis, therefore also called axial diffusivity (AD); the average of λ_2 and λ_3 , the diffusivities along the minor axes, is the radial diffusivity (RD). The fractional anisotropy (FA) and the apparent diffusion coefficient (ADC) were also computed in the defined ROIs. The ROIs used here were the ones previously drawn for the anatomical determinations.

Magnetic resonance spectroscopy (MRS)

The volumes of interest (VOI) with dimensions 4 × 1.5 × 3 mm were placed in the hippocampus or cortex. The non-water suppressed and water-suppressed spectra were acquired using a point-resolved spectroscopy (PRESS) sequence. The water-suppressed acquisition parameters were: TR = 2500 ms, TE = 15.8 ms and averages = 256. The metabolite concentrations (glutamine, Gln; glutamate, Glu; Myo-inositol, Ins; N-acetyl aspartate, NAA; glycerophosphocholine + phosphocholine, GPC+PCh; NAA+NAAG; total creatine = creatine + phosphocreatine, Cr+PCr; and glutamate + glutamine, Glu + Gln), were calculated using the linear combination method LCMoDel (Stephen Provencher

Inc, Oakville, Ontario, Canada). The non-water suppressed signal measured from the same VOI was used as an internal reference for the absolute quantification of metabolites.

Statistical analysis

For the univariate comparisons, all data were processed in NCSS 2007. D'Agostino & Pearson omnibus normality test and Levene's homoscedasticity test were performed. Since not all of the data groups presented normal distribution, the use of a 2-way ANOVA was not possible. Instead, for age and sex comparisons, a *t*-test or Mann-Whitney *U* test were performed depending on the normality assumption. For all cases, $P < 0.05$ was taken as a significant difference between groups. The resultant graphs were performed with the GraphPad Prism 7 software.

Dimension reduction of evoked potential measurements

To reduce the number of variables of evoked potentials used to relate to the redox response, we used principal component analysis to collapse/reduce dimensions into 1 or 2 new variables.

The Brainstem Auditory Evoked Potentials (BAEP) waves I, II, III, IV, and V were reduced into two dimensions henceforth referred to as BEAP I and BAEP II (cumulative variation explained: 93.78%, Dimension 1: EG =4.3, $\text{Chi}^2 = 193.17$, dF =14, $P < 0.0001$; Dimension2: EG =0.38, $\text{Chi}^2 = 48.79$, dF =9, $P < 0.0001$).

The three components measured from Visual Evoked Potentials (VEP), N₁, P₁, and N₂ were reduced to one dimension, henceforth referred to simply as VEP (variation explained: 86.55%, Dimension 1: EG =2.6, $\text{Chi}^2 = 64.33$, dF =5, $P < 0.0001$).

The four components measured from the Medial Nerve Somatosensory Evoked Potential (MNSSEP): CxP1, CxN1, C7P1, C7N1 were reduced to one dimension, henceforth referred simply as MNSSEP (variation explained: 82.50%, Dimension 1: EG =3.3, $\text{Chi}^2 = 101.4$, dF =9, $P < 0.0001$).

The Tibial Nerve Somatosensory Evoked Potentials (TNSSEP): CxP1, CxN1, L4P1, and L4N1 were reduced to one dimension, henceforth referred to simply as TNSSEP (variation explained: 80.3%, Dimension 1: EG =3.3, $\text{Chi}^2 = 133.9$, dF =9, $P < 0.0001$).

Discriminant analysis

The database was tested for multivariate normality with the Doornik and Hansen omnibus test (Ep: 31.20, $P = 0.22$), and for multivariate equal variances we used the Monte Carlo test ($P = 0.057$). To characterize each age/sex group according to their collapsed evoked potentials and redox response, we performed a discriminant analysis. We first used a stepwise variable selection to determine the variables which would significantly contribute to the model. Afterwards, the model was performed using a Linear Discriminant Analysis (LDA).

Regression models

We also explored multiple relationships between the redox response (antioxidant activity, carbonyl content, and redox state) with evoked potentials' collapsed variables.

For the lineal relationships, multiple linear regressions were performed. For non-linear relationships, a neural network analysis was performed; the validation method used was KFold =5 with 3 nodes; the training and validation sets statistics are indicated in each graph. In cases where variables were related to a single variable, univariate linear regressions, and 2nd, 3rd, or 4th order non-linear regressions were performed. All multivariate statistics were performed with the JMP 9 statistic software and the graphs were edited with the GraphPad Prism 7.

Results

SOD and CAT enzymatic activity

The SOD and CAT enzymatic activity was measured in the Cx and the Hc from young and old rats of both sexes. In males, the SOD activity was different in young vs. old animals in both brain regions (Fig. 1A). However, while the enzymatic activity increased in the Cx, in the Hc the activity was lower in the old group compared with the young one. Interestingly, in females, the SOD enzymatic activity in the Cx showed no difference between young and old rats (Fig. 1B), while there was a lower antioxidant activity in the Hc from old animals. When young males and females were compared, a

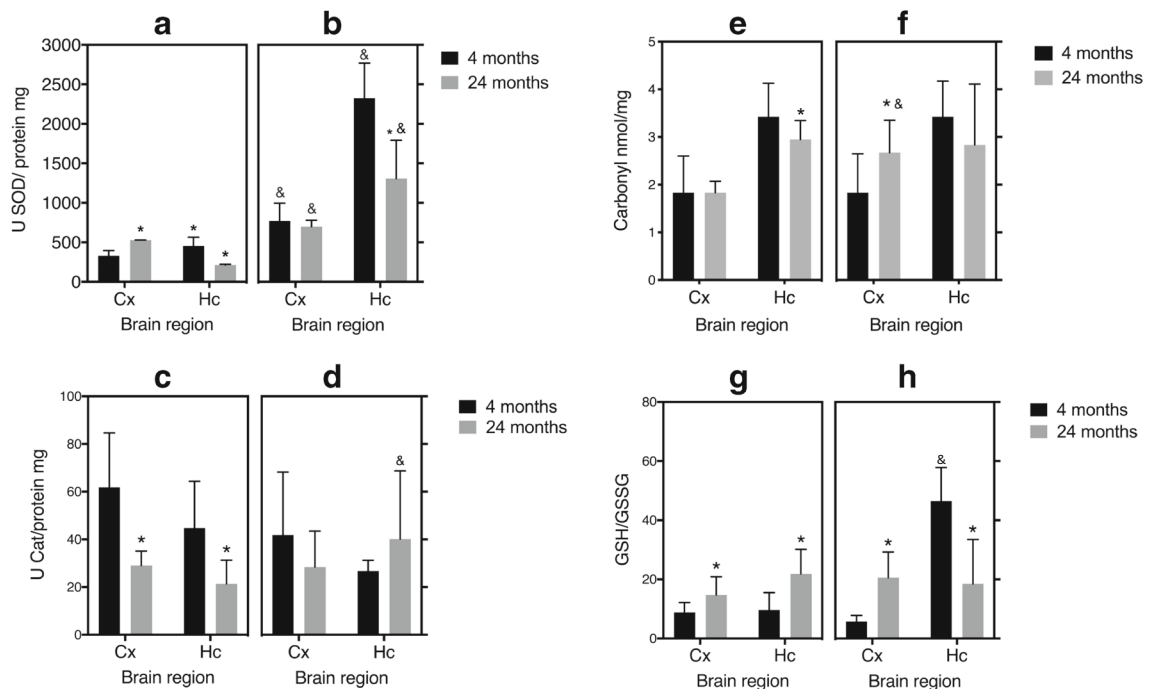


Fig. 1 Biochemical determinations related to redox state. The enzymatic activity of SOD (a–b) and CAT (c–d), as well as the protein oxidative damage (carbonyl content) (e–f) and the GSH/GSSG rate (g–h) [30], was measured in the brain cortex (Cx) and the hippocampus (Hc) from young ($n=10$) and old ($n=5$) female

and male rats as described in materials and methods. The bars represent the mean \pm S.D. of independent determinations, ANOVA followed by Tukey's multiple comparison test. Statistical significance with respect to young animals (*) $P < 0.05$, or between males and females (&) $P < 0.05$ were considered

higher SOD activity was found in females Cx and Hc (2.3-fold and 5.1-fold, respectively). In the case of old males vs. old females, there was a higher SOD activity in both brain regions in females (Cx: 1.4-fold and Hc: 4.1-fold).

Regarding CAT activity, it was observed that old males decreased their enzymatic activity in both brain regions (Fig. 1C). Conversely, in the females, no differences were found in the Cx or the Hc (Fig. 1D). When young females and males were compared, a lower CAT activity in the Hc was observed in females, but no differences between same age groups were noted in the Cx. Conversely, when old groups from both sexes were compared, old females had a higher CAT activity than males in the Hc (2.05-fold), but no differences were found in the Cx.

Carbonyl content

Figure 1E and F shows that the Cx's carbonyl content from old female rats was higher than the carbonyl content in young animals. Curiously, in the Hc, lower

carbonyl amounts were determined. No differences were found in the carbonyl content in the males' Cx but, as well as in old females, a reduction was noted in the Hc from old males. When both sexes' old groups were compared, old females presented a higher carbonyl content in the Cx than old males. In the Hc, old females had lower levels of carbonylated proteins when compared with old males.

Redox state determination

Since the GSH/GSSG ratio is an indicator of the redox state, both compounds were evaluated (Fig. 1G and H). In female and male old groups, the Cx presented a higher GSH/GSSG ratio when compared with the young groups (3.5- and 0.69-fold respectively). In contrast, in the Hc, the GSH/GSSG ratio differed between males and females. While in females the GSH/GSSG ratio decreased with age, in males, a higher ratio was observed in the older group (2.2-fold compared with young males).

No differences in the redox state in the Cx were observed between sexes. Female and male groups obtained similar GSH/GSSG ratio values, showing an age-related increase. In the Hc, the redox state was not different between 24-month-old females and males. Interestingly, in the Hc, 4-month-old females showed a higher GSH/GSSG ratio than same age males (4.8-fold).

Neurophysiological assays

Brainstem auditory evoked potentials (BAEP)

The evaluation of the left and right auditory latencies waves I, II, III, IV, and V from young and old rats of both sexes are shown in Fig. 2A, B, and C. The representative images of BAEP wave measurements are shown in Fig. 2A. In females, all waves significantly increased their latency with age (Fig. 2C), while in old males only, the latencies in waves III and V were significantly higher than in the young group ($P < 0.05$, Fig. 2B). Furthermore, longer latencies were recorded in young males when compared with young females in waves I, II, III, IV, and V ($P < 0.05$, Fig. 2C). Interestingly, no differences between groups were found when old males were compared to old females.

Visual evoked potentials (VEP)

The N1, P1, and N2 waves of the visual pathway were evaluated and the representative images of VEP wave measurements are shown in Fig. 2D. The latencies of all waves evaluated in both males and females were higher in old animals than in young animals ($P < 0.05$). The increase in old males (Fig. 2E) was 3.2 ms in the N1 wave, 8.2 ms in the P1 wave, and 9.4 ms in the N2 wave. While in old females (Fig. 2F), the increment was 5.5 ms in the N1 wave, 3.8 ms in the P1 wave, and 5.4 ms in the wave N2. No differences were found between the latencies of young males and young females, but when the old males were compared with the old females, lower latencies were recorded in the P1 and N2 waves of old females.

Medial and tibial somatosensory evoked potentials (MSSEP and TSSEP)

The P1 and N1 waves of the somatosensory cortex (Cx) and the cervical disk (C7) were evaluated for MSSEP

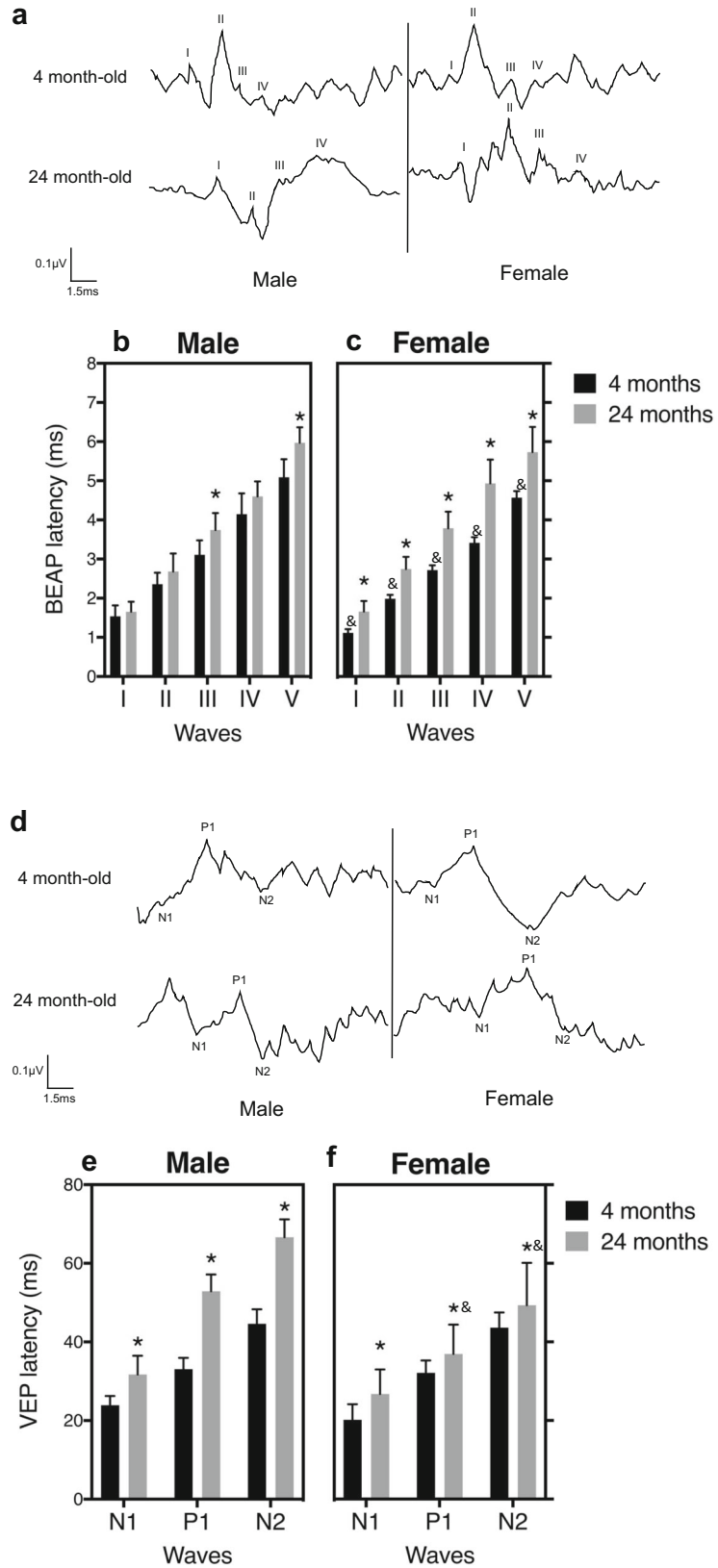
Fig. 2 Neurophysiological assays. **(a)** Brainstem auditory evoked potentials (BAEP). The figures in a represent the morphology of the auditory pathway waves (I–V) determined in female and male rats in each age group. The BAEP were obtained as described in Materials and Methods in **(b)** young ($n=10$), and old male rats ($n=5$), and **(c)** young ($n=10$), and old ($n=5$) female rats. **d–f.** **(d)** Visual evoked potentials (VEP). The three components of the visual pathway (N1, P1, N2) are observed in female and male rats in each age group. The VEP were obtained as described in materials and methods in **(e)** young ($n=10$), and old male rats ($n=5$), and **(f)** young ($n=10$), and old ($n=5$) female rats. **g–i.** Medial somatosensory evoked potentials (MSSEP). In **(g)**, the morphology of the MSSEP waves is shown in both males and females young and old rats. The electrical activity of the anterior limb somatosensory pathways in **(h)** young ($n=10$), and old male rats ($n=5$), and **(i)** young ($n=10$), and old ($n=5$) female rats was determined. The CxP1, CxN1, C7P1, and C7N1 waves were obtained as described in materials and methods. **j–l** Tibial somatosensory evoked potentials (TSSEP). In **(j)**, the morphology of the MSSEP waves is shown in both males and females young and old rats. The electrical activity of the posterior limb somatosensory pathways in **(k)** young ($n=10$), and old male rats ($n=5$), and **(l)** young ($n=10$), and old ($n=5$) female rats was determined. The CxP1, CxN1, L4P1, and L4N1 waves were obtained as described in materials and methods. The bars represent the mean \pm S.D. of independent determinations. An ANOVA test was performed, followed by Tukey's multiple comparison test. Statistical significance to young animals (*), or between sexes (&), $P < 0.05$ were considered

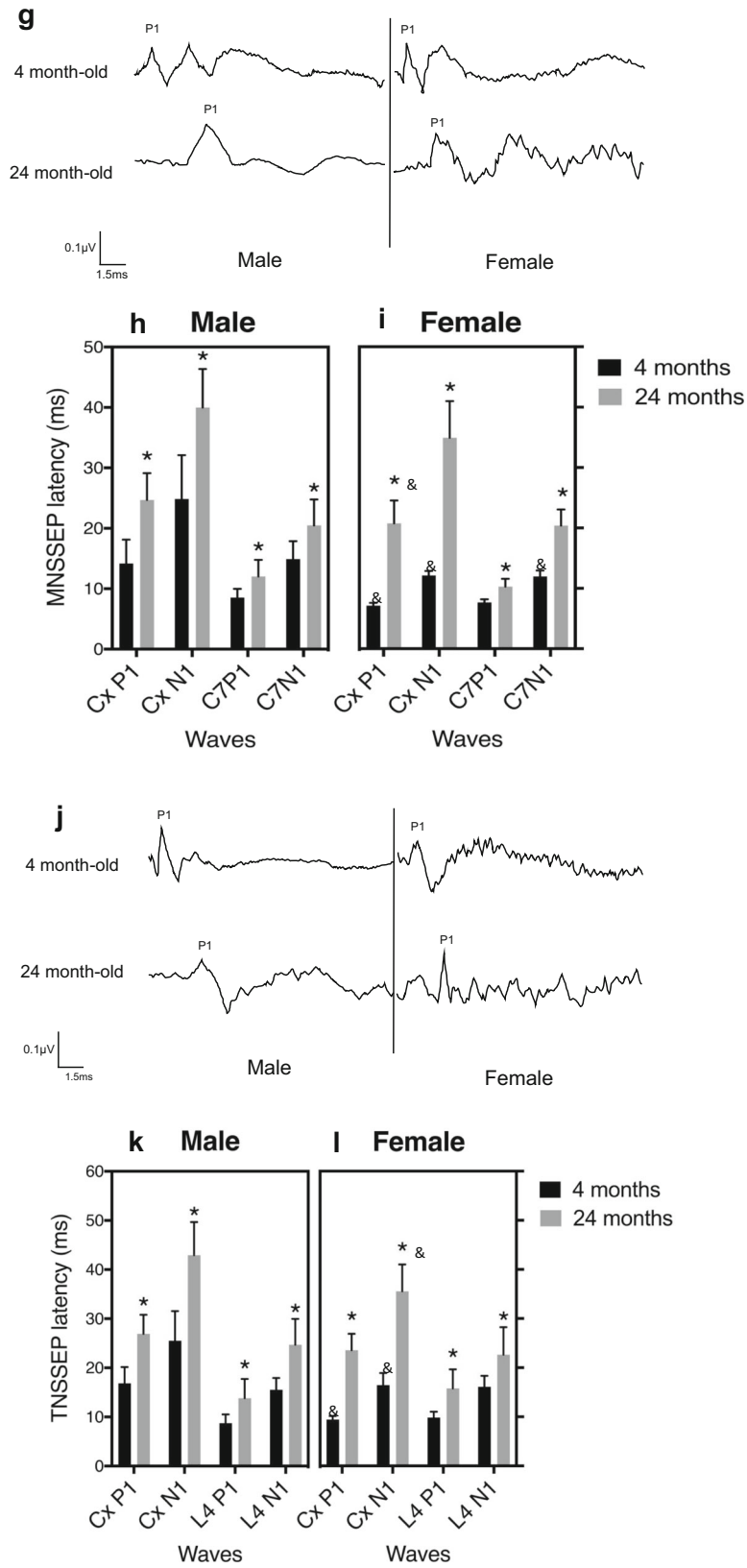
(Fig. 2G), while the P1 and N1 of the Cx and the Lumbar 4 derivation (L4) were evaluated for TSSEP (Fig. 2J). The latencies of all evaluated waves in both males and females were higher in old animals than in young animals ($P < 0.05$). In the case of the TSSEP, a similar behavior was observed (Fig. 2K and L).

Higher latencies in the CxP1, CxN1, and C7N1 waves from MSSEP were found in young males compared with young females ($P < 0.05$). In old groups, the differences were lost in almost all waves, except for the CxP1 wave in which the latencies were longer in males (Fig. 2H and I).

Regarding to TSSEP, the CxP1, and CxN1 were longer in young males compared with same-age females ($P < 0.05$), similarly as in MSSEP. Finally, in females and males old groups, the same behavior as in MSSEP was observed in TSSEP. The differences were lost in almost all waves, except for the CxN1 wave, in which longer latencies were recorded in old males compared with old female rats.

In summary, the evoked potentials performed in the old animals showed higher latencies in the different





waves evaluated, pointing towards a decrease in the nerve conduction velocity during aging.

Discriminant and regression analysis of antioxidant parameters and evoked potentials by sex and age

In order to determine the differences between the experimental groups, a discriminant analysis was performed using the covariates corresponding to the redox response (enzymatic activity, carbonyl content, and redox state), along with the evoked potentials. The MR and NOR data were not included because the first ones were performed only in females, and the second ones were not paired. In Fig. 3, each point represents an individual in each of the four experimental groups, and the circles indicate the region where most of them are grouped. The fact that all the circles are separated indicates that all the groups behaved differently. The circles were colored to indicate experimental groups. The biplot represents the variables projected on lines or rays in the graph, with different ray lengths depicting the importance of the variable, the larger the ray is, the greater the importance of the variable. The discriminant analysis between age and sex groups was performed only using the covariates, which significantly contributed to the model ($P < 0.05$): GSH/

GSSG-Cx, SOD-Hc, SOD-Cx, CAT-Hc, CAT-Cx, MNSSEP, and TNSSEP evoked potentials.

The model was significant (Wilks' lambda = 0.0005, $F_{18,51} = 15.69$, $P < 0.0001$), and both canonical dimensions explained 95.9% of the total variance. The relationship between antioxidant and EP was remarkably different for each group, highlighting that female and male physiological responses differ as they age.

In the case of the young females, the EP results were positively related to the early scavenger barrier SOD, but negatively to the H_2O_2 scavenger CAT. They were also positively related to protein damage and negatively related to the redox state (Supplementary Fig. 1). While in the old females, EP were mostly positively related to CAT (Supplementary Fig. 2). The majority of EP obtained from old females were not directly related to protein damage, except for VEP that was related to the Cx carbonyl content.

The evoked potentials in young males were highly related to the GSH/GSSG ratio, but the relationship was not the same for all of the evoked potentials assessed. For example, when TNSSEP and BAEP II were high, the GSH/GSSG ratio was also high; however, when MNSSEP and VEP were high, the GSH/GSSG ratio was low (Supplementary Fig. 3). Although, compared to young females, young males-EP were more related to carbonyl content; moreover, they were also positively

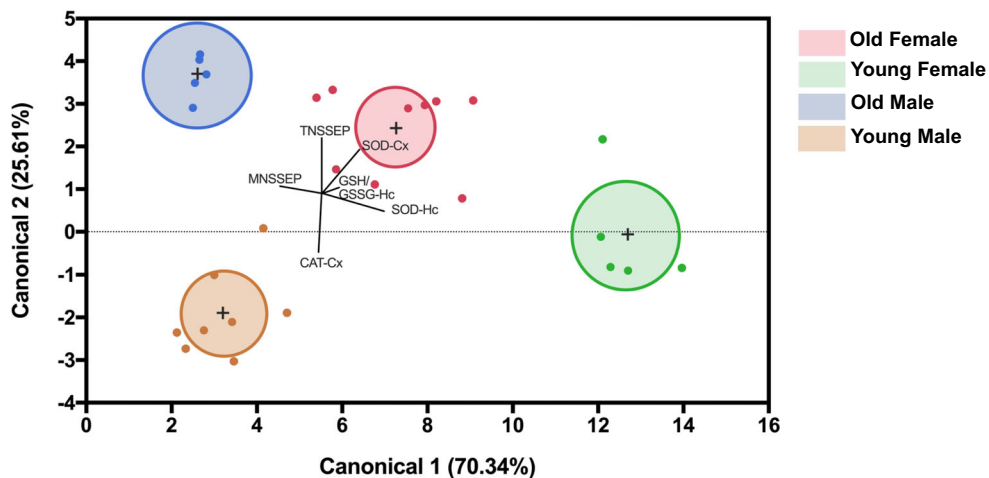


Fig. 3 Linear discriminant analysis plot. The Canonical Plot shows first (x-axis) and second (y-axis) canonical dimensions. This represents the covariates linear combination (antioxidants and evoked potentials) that maximizes the multiple correlation between the category (experimental groups) and the covariates. The experimental groups are represented by a 95% confidence level ellipse and each group mean is denoted by a plus (“+”) marker. The percentage of variation explained by each canonical

dimension is indicated. If two groups differ significantly, the confidence ellipses avoid to intersect. Each ellipse has a different color to facilitate its distinction. The set of rays that appears in the plot represents the covariates that are significantly contributing to separate each group. The length and direction of each ray in the biplot indicate the degree of association of the corresponding covariate to the classified groups

related to the antioxidant activity as a mechanism of compensation.

Finally, evoked potentials of old male rats were mainly associated to the CAT activity and the redox state, as well as to the carbonyl content, mainly in the Cx. Though, when compared to old females, old males' EP were more related to protein damage. The carbonyls decrease coincided with the antioxidant activity (Supplementary Fig. 4). When comparing old vs. young males, the relationships shifted from linear to non-linear, since there were less antioxidant enzymes involved. Furthermore, compared to young males, in old rats, only individual relationships between evoked potentials and specific antioxidants were observed, while in young male animals, the antioxidants had a combined influence over the evoked potentials.

Novel object recognition test

To assess the potential detrimental effects of the sensory deficits detected by the EP upon cognition, a novel object recognition test was performed in both young and old, as well as male and female rats. As shown in Fig. 4A, young animals spent more time exploring the new object as compared to the old object; they also presented more interactions with the new object as compared to the known object (Fig. 4B). The 4-month-old female and male rats spent more than 80% of the exploration time exploring the new object. Meanwhile, old rats spent overall less time exploring both objects as compared to same sex young animals (Fig. 4C). In addition, old male and female rats were incapable to discriminate the new object from the previously presented one, as depicted by the low preference index (Fig. 4D) and by the small period of time exploring the new object (Fig. 4A), and the low interaction number (Fig. 4B). Although old females had a trend to explore the novel object for longer periods and more times, this difference did not reach a level of significance.

Diffusion tensor imaging (DTI)

Fractional anisotropy (FA) (Fig. 5A), as well as axial (AD) and radial diffusivity (RD). (Fig. 5B and C), were evaluated in the brain cortex (Cx) and the hippocampus (Hc) of young and old female rats. All MRI/MRS determinations were not possible to perform in old male

rats, because the great size they reached as they aged hampered introducing them inside the 7 Tesla resonator. Hence, these experiments were performed only on females. The overall diffusivity (i.e., AD and RD) was reduced in the cortex of the 24 month-old rats, as compared to the young animals, with no change in FA. In the hippocampus, RD was reduced, while AD showed no differences between the young and old animals, conditioning an increase of FA in this region. The decrease in AD and RD produced a significant apparent diffusion coefficient (ADC) reduction in both brain regions (Fig. 5D).

Volume measurement of brain structures by magnetic resonance imaging

The volumes of Hc and Cx were also determined since they are two of the most damaged structures during aging. Supplementary Fig. 5 is a representative image that shows the ROIs where the measurements were obtained. No significant differences were found in the Hc volume with age (Fig. 6A), but there was a significant decrease of 14.6% in the Cx volume of old rats compared with the 4-month old group (Fig. 6B). The total brain volume was also measured, and a significant decrease of 8.11% was found in old rats compared with the young group (Fig. 6C).

Metabolites quantification by MRS

In order to obtain a more detailed scenery of brain alterations during aging, several brain metabolites were evaluated. We were only able to obtain *in vivo* ^1H NMR spectra from the female rats since the old males were too large to fit into the animal scanner. The representative MR spectra are shown in Fig. 7A. The water signal was well suppressed, and the signal-to-noise was 7.5 ± 1.7 Hz and 8.0 ± 1.9 Hz in the spectra from the Hc and the Cx respectively. Only the metabolites with CRLB below 20% were considered. The complete results are shown in Supplementary Table 1, and as observed, the quantified metabolite levels were higher in the Cx than in the Hc at both, 4 and 24 month of age (Fig. 7B), in particular Glu, NAA, NAA+NAAG, and total creatine. In the Hc of old female rats, a decrease in the neuronal marker NAA and an increase in the Myo-inositol levels ($P < 0.001$) were observed when

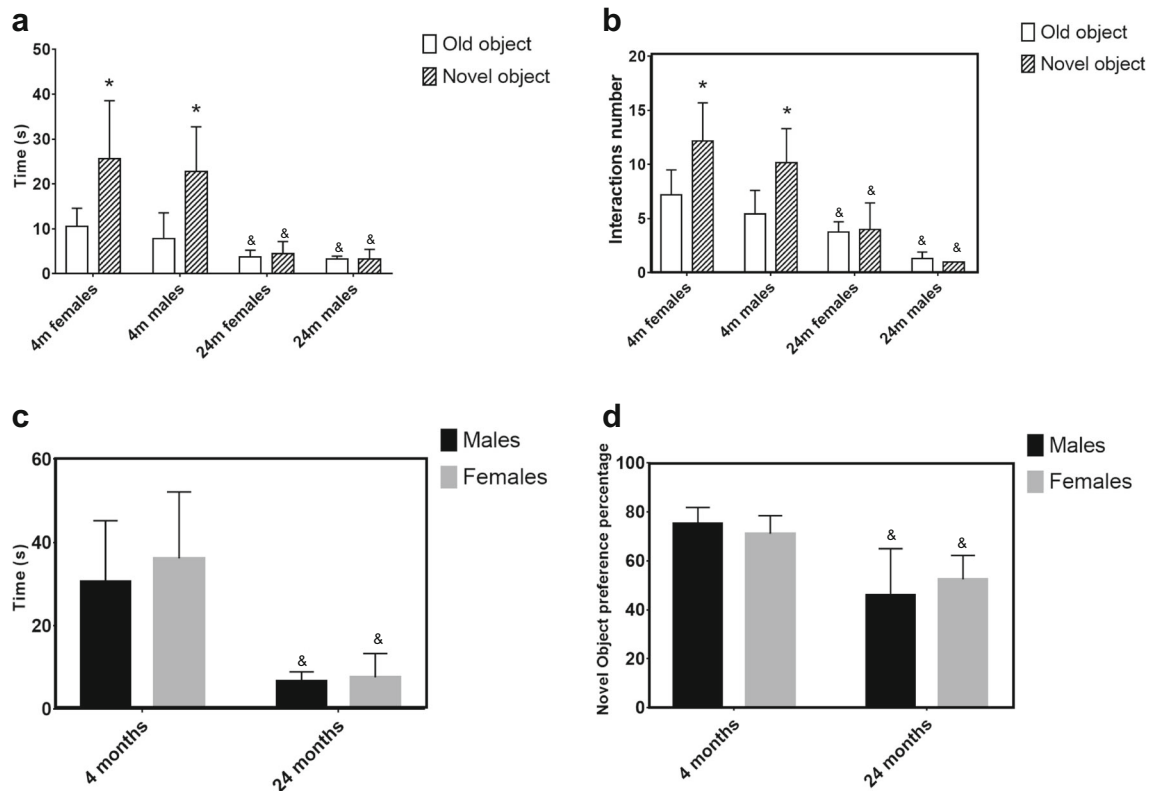


Fig. 4 Novel object recognition test. New and old object interaction time (**a**) and number (**b**) were determined in young ($n=12$), and old male rats ($n=3$), and young ($n=10$), and old ($n=4$) female rats as described in materials and methods. Young animals from both sexes showed a higher number of interactions and interacted more time with the new object as compared to the old object. Old animals did not discriminate between them. Mann-Whitney U test. (*) $P<0.05$ as compared with the old object; (&) $P<0.05$ as compared with same sex young group. No differences between sexes were noted. Total exploration time (**c**) was also determined in young ($n=12$), and old male rats ($n=3$), and young ($n=10$), and

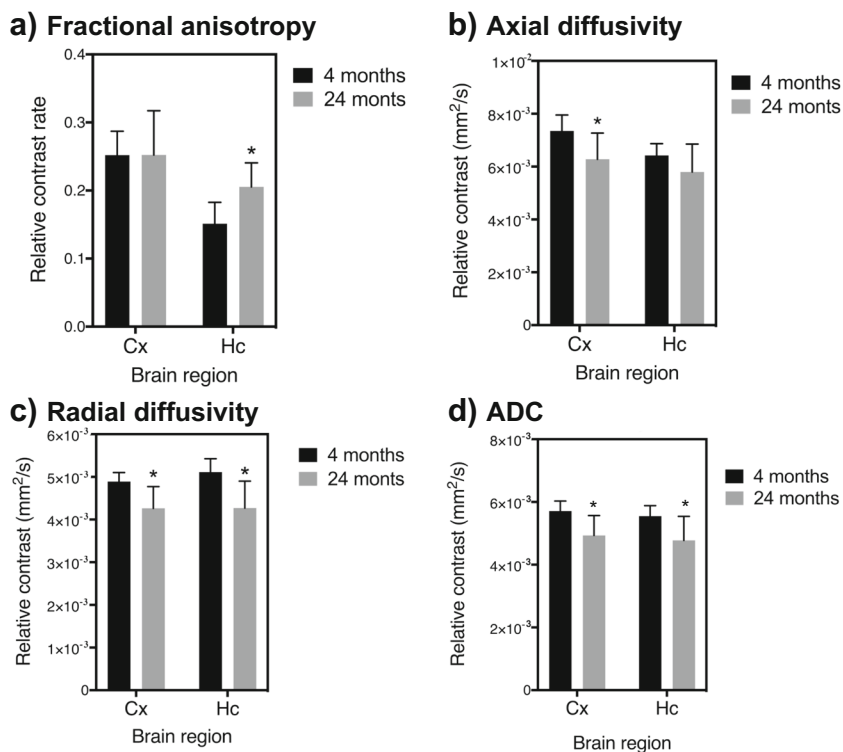
old ($n=4$) female rats and it showed that old animals spent less time interacting with the objects as compared to young animals. The Preference index was calculated dividing the time spent exploring the novel object by the total exploration time multiplied by 100, in order to obtain a percentage value (**d**), this index indicated that young animals spent more than 80% of the interaction time exploring the new object, while the old animals did not discriminate between the new and old objects, as they spent approximately 50% of the exploration time interacting with the new object. Mann-Whitney U test; (&) $P<0.05$ as compared with the young group. No differences between sexes were noted

compared with young rats ($P < 0.05$). Contrastingly, metabolite levels in the Cx were not different, but the ratio (Glu+Gln)/(Cr+PCr) diminished with age. Pearson correlation coefficients (r) were calculated to find a possible linear dependence between the measured metabolite levels. As shown in Supplementary Fig. 6A, there was a positive linear dependence between several metabolites measured in young animals. Interestingly, the Cx metabolites displayed a greater dependence on each other than the metabolites determined in the Hc. Remarkably, in aged rats' brains, the dependency between metabolites in both regions seemed to be disrupted (Supplementary Fig. 6B).

Discussion

Sex differences in neurophysiology are considerable and might be influenced by multiple features, from anatomical to molecular levels. Most of the studies involving sex differences in the nervous system are performed in young individuals, so, normal age-related changes are usually not evaluated. Additionally, to date, most of the behavior studies are still done in males, although it is already known that females and males age differently. Thus, it is important to analyze the alterations during the aging process in the nervous system's physiology and morphology. Generally, these differences are attributed to hormonal changes [31]. However, it has been accepted that

Fig. 5 Diffusion tensor imaging (DTI). Brain MR quantifications. Fractional Anisotropy (FA) (a), Axial Diffusivity (AD) in mm^2/s (b), Radial Diffusivity (RD) in mm^2/s (c), Apparent Diffusion Coefficient (ADC) in mm^2/s (d). The bars represent the mean \pm S.D. of independent determinations. ANOVA test was performed, followed by Tukey's multiple comparison test. A statistical significance with respect to young rats (*) $P < 0.05$ was considered



there may be other factors, such as oxidative stress, that might be involved in the dissimilar brain deterioration between sexes [31, 32].

The oxidative stress theory of aging, proposed in the 1950s by D. Harman [33], postulated that macromolecule oxidative damage accumulation, due to oxygen free radicals formed from normal metabolism caused aging

deterioration. Nevertheless, in the last decades, this theory has been widely debated because numerous experiments conducted on transgenic/knockout animals, for a wide variety of antioxidant enzymes, had shown no effects on lifespan [14]. Therefore, oxidative stress was not included in the nine hallmarks of aging described by [1]. Nevertheless, it has been argued that

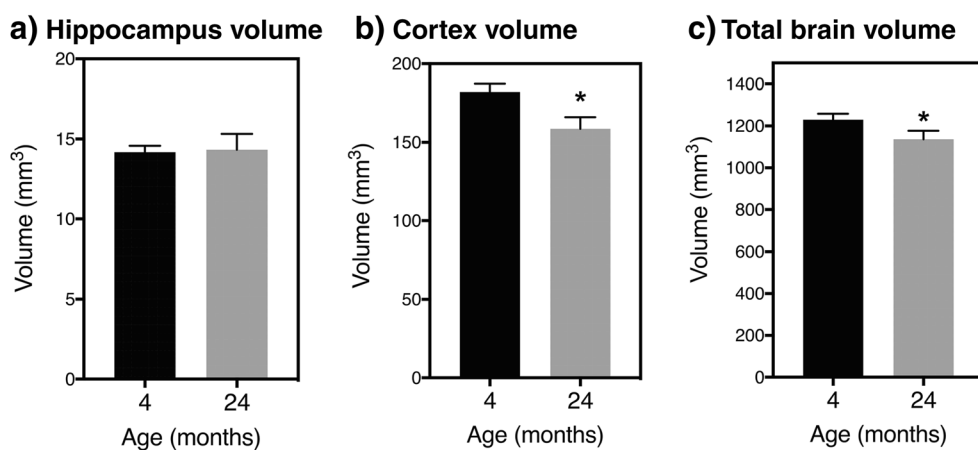


Fig. 6 MR imaging volume quantification. Volume measured in the hippocampus (Hc) (a), cortex (Cx) (b), and whole brain (c) of young ($n=10$) and old ($n=5$) female rats. The bars represent the mean \pm S.D. of independent determinations. ANOVA test was

performed, followed by Tukey's multiple comparison test. Statistical significance with respect to young rats (*) $P < 0.05$ was considered

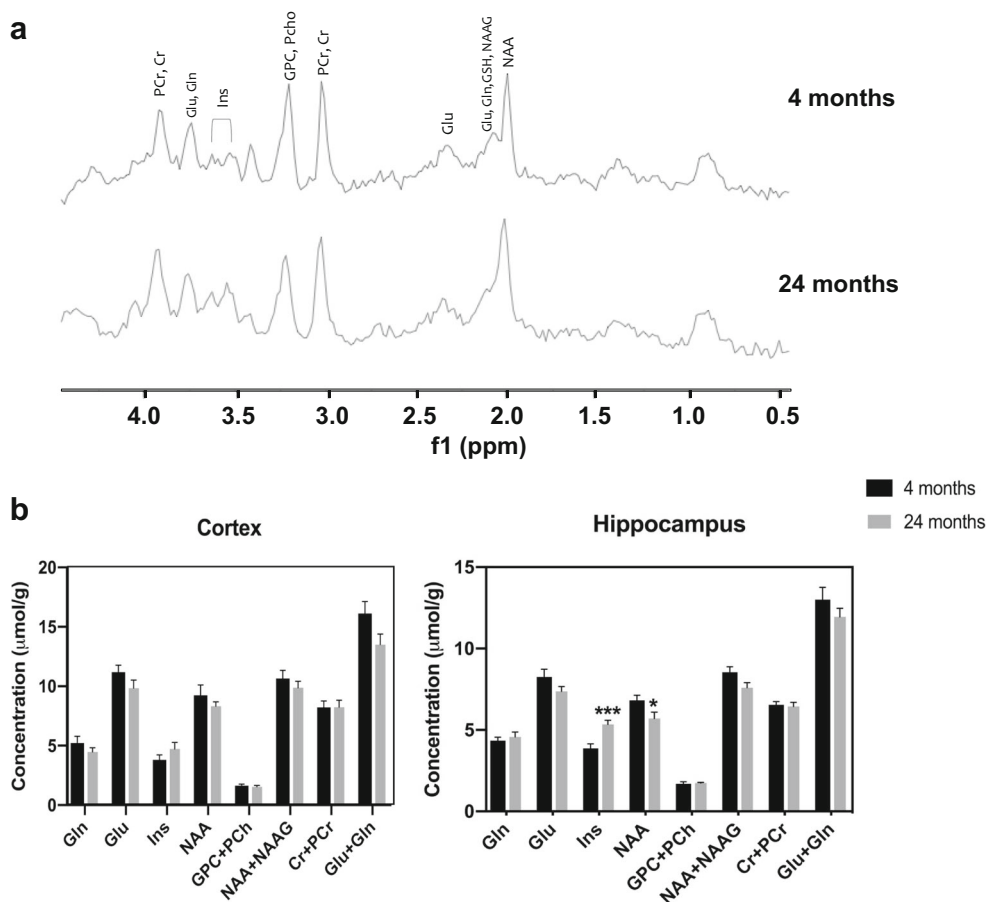


Fig. 7 Metabolite quantification by MRS. **a** Representative MR spectra from the hippocampus of 4- and 24-month-old female rats acquired in vivo with PRESS at 7T as described in the Materials And Methods section. The Ins (Myo-inositol) peak shows a higher intensity in old rats. **b** Metabolite concentration in the Cx and Hc of 4- and 24-month-old rats female rats. Abbreviations are as follows: glutamine, Gln; glutamate, Glu; Myo-inositol, Ins; N-acetyl aspartate, NAA; glycerophosphocholine + phosphocholine,

GPC+PCh; NAA+NAAG; total creatine = creatine + phosphocreatine, Cr+PCr; and glutamate + glutamine, Glu + Gln. Metabolite concentrations were calculated using the linear combination method LCModel (Stephen Provencher Inc, Oakville, Ontario, Canada). Statistical significance with respect to young animals (*) $P < 0.05$, (***) $P < 0.001$ were considered. The complete results are shown in Supplementary Table 1

the redox metabolome and proteome serve as adaptive interfaces for genome–exposome interactions that modulate the hallmarks of aging, and therefore changes in the redox state might be considered when studying the aging process [34]. Kunath and Moosmann (2020) [35] have recently proposed that the discrepancies in validating or invalidating this theory rely on the rate-limiting kinetic steps of the aging cascade, and that the disagreements arose depending on the time when the experiments were done, i.e., radical propagation vs. radical initiation or termination; because, apparently, radical propagation might be the rate-limiting step for aging and this step has barely been studied. Though, regardless of whether or not oxidative stress governs

longevity, its participation in the normal and pathological brain deterioration is of great relevance [15], Oxidative stress is known to be a mechanism for age-related brain functional decline [36, 37]. So, the way in which each of the sexes handles oxidative stress to reach redox homeostasis could be a factor that influences the way in which the brain ages in males and females.

The cerebral cortex (Cx) is a high-level processing structure that has been associated with somatosensory processing information [38], meanwhile the hippocampus (Hc) is responsible for numerous cognitive functions, such as learning and memory processes [39]. Oxidative damage in the Hc and the Cx has been associated with cognitive decline [40] and

therefore, the redox state was evaluated in these two brain regions to understand the oxidative stress role in nerve conduction velocity's and memory dysfunction during aging.

The biochemical determinations related to the redox state revealed interesting results. A higher SOD activity was found in females' Cx and Hc compared to males regardless of the age. This difference is consistent with what has been reported for young females in murine models [41–44], and has been associated with the levels of sex hormones, mainly progesterone and estrogen [31, 45]. There are very few studies regarding SOD activity in old murine females, but it appears that the activity decreases together with the sex hormones decline [31]. Moreover, our results showed a significant decrease in SOD activity in the Hc of both sexes during aging coinciding with other reports [46]; remarkably, augmented oxidative stress within the Hc has been associated with age-related cognitive decline and somatosensory function [47].

CAT activity in males significantly decreased with age in both brain regions, concurring with Guevara's work [46], which reported that CAT activity declined with age in Wistar rats, regardless of their sex. Here, we also did not find significant differences by sex, and CAT activity showed high variability in females. In other reports where CAT activity was evaluated in the normal brain and in dementia murine models [48] no sex-related differences were found.

Regarding the GSH/GSSG ratio, there was an increase in males with age in both brain regions, while in females, the increment was only observed in the Cx, and no differences were found between sexes during aging. Therefore, the evidence comparing the GSH system and the redox status in the brain from female and male rodents is still inconclusive [44, 49]. Increased GSH levels have been observed in adult male rats exposed to Pb-induced oxidative stress with hippocampal damage and impaired memory [50]. This effect might be related to a compensatory mechanism to reestablish redox homeostasis.

Apparently, females have a better management of the redox state. In this sense, Guevara's group [46], who also found no differences in the antioxidant enzyme activity between old male and female rats, proposed that the reason why old female rats seemed to have better redox homeostasis is due to better mitochondrial functionality, and not just antioxidant activity. That idea would be very worthy to analyze in the future.

Differences in nerve conduction velocity have been evaluated in human males and females, and the results

have shown that males have higher latencies in somatosensory [51, 52], visual [53, 54], and auditory pathways [55, 56]. This observation seems to be maintained in other mammals like rodents and non-human primates, in which latencies increase with age, and nerve conduction velocity decreases, but the magnitude varies between sexes [12, 57]. Here, we also found sex-dependent variations in nerve conduction, with longer latencies recorded in males during young and adult stages, concurring with other authors, and pointing towards a systemic nerve conduction impairment and electrophysiological alterations during aging [58]. Our data support that latencies augment with age in both sexes in all evaluated sensory pathways, in a similar way as in humans, suggesting comparable mechanisms of deterioration in old individuals. Even though we registered longer latencies in male rats since youth, when compared with same-age females, these significant differences between sexes were lost in the old groups, with the exception of the visual evoked potentials (VEP), where old females presented lower latencies in the P1 and N2 waves than old males. Interestingly, it has been reported by Kuba and co-workers [59] that the differences in N2 peak latencies may not be entirely attributable to different parameters of motion stimuli, but also to differences in the age of subjects, and that VEP latencies prolongation might be a good indicator of individual biological aging.

The decrease in age-related conduction velocity has been associated with the myelin loss or the deterioration associated to oxidative stress [60, 61]. Some authors suggest that these effects could be a consequence of the loss of thickness and number of myelinated fibers during aging, leading to neurophysiological impairment [62]. Our aforementioned data, regarding the increase in oxidative stress with age, support this idea, since oxidative damage also triggers neuronal injury and cell death [36]. Oxidative stress might be related to mitochondrial dysfunction, high iron levels, decreased antioxidant enzymes, altered Ca^{+2} homeostasis, microglial activation, etc. [15, 63, 64]. All these features, along with other changes in the neuronal excitability related to metabolism, such as channel protein levels and activation, as well as membrane composition modifications, might influence the conduction velocity observed during the EP and should not be put aside [65].

To improve the understanding of the relationships between age and sex, we performed a discriminant analysis to integrate several parameters (enzymatic activity, protein damage, and GSH/GSSG) with the functional

response of evoked potentials. The discriminant analysis revealed a non-linear relationship between oxidative stress and EP in young female rats, where the increase in the latencies coincides with a rise in carbonyls and the reduction of the redox state, suggesting that there might be an association between damage and nerve pathway dysfunction. Interestingly, this behavior only occurs up to a certain threshold, since, when reaching certain slowness in the EP (particularly in MNSSP), this relationship is reversed, improving the redox status and the latencies. These results could explain why young females possibly activate redox protection mechanisms to prevent the somatosensory pathway deterioration.

However, in old female rats, the SOD activity decreased and the CAT remained the same, so their effect might be insufficient to clear all the ROS generated. Hence, the activity of the two enzymes might be insufficient to avoid protein damage, which also concurs with the decrease in the conduction velocity. Interestingly, both, young and old females, had higher SOD activity than males; however, with age this was not enough to prevent age-associated damage.

The regression analysis showed a direct relationship between the GSH/GSSG ratio and the EP in young rat males, suggesting that maintaining a reduced redox state could favor the somatosensory pathway's functionality. When the EP of males are compared with those of females, it is observed that, although there is a greater relationship with protein carbonylation, there is also a high enzymatic activity, possibly as a compensation mechanism. In the case of old males, the regression analysis revealed a relationship between the decrease in the redox state and the activity of antioxidant enzymes, with the increase in the latencies and protein damage, especially when compared to young males. Although compared with old females, it seems that when females age, they can cope with the damage better than males, since more relationships were found between increased latencies and carbonyl damage in old males than in old females. Furthermore, in old females, the models were multivariate; in most cases, the EP were related to the antioxidant parameters simultaneously, while in old males, each comparison was independent of the previous one.

Memory tests involve the detection of various sensory inputs (visual, somatosensory, and probably auditory and olfactory) in order to integrate the information about space and their subsequent comparison with previously used stimuli, consequently, the NOR-test was used as a

complementary measure of sensory alterations detected through EP. In addition, there are several studies in rodents where oxidative stress induction by different stimuli negatively impacted cognition [40, 66–68]. The NOR-test showed that old male and female rats were incapable to discriminate the new object from the previous one, and though old females had a greater tendency to explore the novel object, this difference did not reach a level of significance. Therefore, although these results suggest that there is a cognitive decline associated with age, it will be necessary to corroborate them using a larger number of animals.

Unfortunately, most of the studies that evaluate age-related cognition decline are carried out only in males [66–68]. This problem was elegantly discussed by Hernández and coworkers (2019) [7] in a recent paper where they remark that, in addition to the shortage of sexual dimorphism studies related to cognitive decline, there are discrepancies between them that might be explained due to sensorimotor impairments. Their results showed that the old female rats performed significantly better in the rotarod test but that there were no differences by sex in terms of cognitive assessment. Another very interesting study by Logan et al. 2019 [69], using a mice model deficient in the antioxidant enzyme Cu/Zn-superoxide dismutase, provided important evidence that hippocampal oxidative stress alone is sufficient to induce neuroinflammation and age-associated memory decline. In that study, male and female data were analyzed separately and no clear differences between them were reported.

The conduction velocity depends on the suitable functionality of the myelin sheaths, an increase in oxidative stress might oxidized them, impairing their function and, inevitably, affecting memory and cognitive performance. Hence, DTI studies were performed, to obtain information about the integrity of nerve fibers and myelination, in order to evaluate if the changes in the redox state were related to the decrease in the conduction velocity, and if these were associated to myelin loss or degeneration. DTI is a widely used technique to study white matter integrity and to relate it with cognitive disorders and neurodegeneration [20, 70, 71]. These experiments were performed only on females since the old males were too large and did not fit into the scanner. Our results showed a decrease in ADC in the Cx and Hc in old animals, which has been related with cellular swelling, reduced extra-cellular space, astrocytes functional and morphological changes, and extracellular matrix modifications [30, 72, 73]. Neuronal cell death, glial

proliferation, and astrogliosis have also been linked to ADC reductions [74, 75]. In the Hc, an increased FA was observed in old animals, which contrasts with previous reports of reduced anisotropy in CA3 and dentate gyrus of aged rats. The current resolution of our images precluded accurate segmentation of the hippocampal subfields, which may display different patterns of diffusion changes [73]. In addition to the differential effects of aging on hippocampal subfields, this FA increase should be cautiously interpreted, given the low diffusion anisotropy typical of gray matter, and the susceptibility of FA to noise in the low anisotropy regime [76]. The ADC data indicate that inflammation, probably generated by the glia, is an important factor that also contributes to myelin deterioration. It is widely documented that oxidative stress induces neuroinflammation [77]. Changes in ADC have also been interpreted as microstructural changes in the brain [78, 79] and reduced ADC has been reported with increasing frequency [30, 72, 73]. Therefore, it was interesting to evaluate brain volume using MRI. The brain volume is known to reduce during normal aging, but the variations do not occur uniformly in all brain regions [80]. Our data support brain atrophy during the aging process because we found a significant reduction in female's brain volume and, in particular, in the Cx, and a trend in the same direction in the Hc volume. Age-related brain atrophy is generally observed in old mammals [80], and a positive correlation between brain volume loss, aging, and cognitive decline has been reported [81]. It has been suggested that grey matter is prone to shrink with age since adulthood, while white matter frequently presents changes at a microstructural level during aging [82]. Hamezh et al [81] reported the effect of age on specific brain region volumes, cognitive and locomotor performance, and antioxidant enzyme activity in adult and old Sprague-Dawley male rats. Although in their study the MDA content increased, no significant changes were observed in the protein carbonyl content with age, moreover CAT and SOD activity were unchanged, while GPX decreased, which led them to conclude that increased oxidative stress along with the shrinking of several brain regions, were among the apparently causative factors of aging associated to cognitive and locomotor decline, as well as the decrease in nerve conduction velocity.

Brain metabolite alterations during aging have been related to the changes in ADC measurements [72] and

might also be involved in cognitive decline. Therefore, the ADC reduction observed during aging might be associated with morphological and physiological changes in the astroglia and the increased secretion of macromolecules to the extracellular matrix. To support this idea, ^1H -MRS was used to quantify the molecular concentrations of some brain metabolites, which have biological relevance, such as glutamine, glutamate, Myo-inositol, N-acetyl aspartate (NAA), glycerophosphocholine, and creatine. In particular, NAA and Myo-inositol are considered neuronal and glial markers, respectively [83, 84]. Our data showed a high correlation between the content of several metabolites in both, the Cx and Hc of young rats. This correlation is disrupted in old animals, which evidences the loss of brain homeostasis and might be related with the age associated brain dysfunction.

Moreover, a significant decrease in NAA levels in the Hc of old female rats was determined. NAA low levels have been correlated with neuronal loss or functional reduction [83, 85], so its decrease in the Hc might be directly associated to the observed age-related cognitive decline. Another interesting finding was a 36% increment in the Myo-inositol levels in the Hc of old rats. There is evidence that correlates high Myo-inositol concentration with pathological astrogliosis during aging, and therefore this metabolite has been considered a glial marker related to neuroinflammation [86–88].

In summary, our results showed moderate dissimilarities regarding memory and nerve conduction velocity by sex, but the differences regarding the redox status could help explaining why the response to different interventions is so dissimilar between males and females. The integration of these results suggests that females seem to cope with neural damage better than male rats. The MRI/MRS results indicated that during normal aging, the deficient response to oxidative stress is coupled with neuroinflammation, which might be aggravating the functional decline; however, these effects related to female results must be confirmed in male animals.

Finding the differences in female and male brain-decline during normal aging is important because, not only are longevity and quality of life different, but also the incidence of various age-related neurodegenerative diseases shows a sex-dependency, along with dissimilar clinical manifestations and drug responses depending on the sex, which influence the diverse responses to treatments [89]. Furthermore, this information is essential to decide where to direct the interventions, in order to

avoid aging deterioration, since what could benefit females is not necessarily the same for males.

Supplementary Information The online version contains supplementary material available at <https://doi.org/10.1007/s11357-021-00353-x>.

Acknowledgements The authors would like to thank Dr. Guerrero-Aguilera from UAM-I for animal supply. This work was supported by Consejo Nacional de Ciencia y Tecnología (CONACyT) grant FON.INST/298/2016, as well as the “Red Temática de Investigación en Salud y Desarrollo Social” from CONACYT. Santín-Márquez R. and Toledo-Pérez R. are CONACyT scholarship holders. Ramírez-Cordero B, Hernández-Arciga U, and Pérez-Morales M. were PRODEP postdoctoral fellows.

Code availability Not applicable

Funding This work was supported by Consejo Nacional de Ciencia y Tecnología (CONACyT) grant FON.INST/298/2016, as well as the “Red Temática de Investigación en Salud y Desarrollo Social” from CONACYT. Santín-Márquez R. and Toledo-Pérez R. are CONACyT scholarship holders. Ramírez-Cordero B and Hernández-Arciga U are PRODEP postdoctoral fellows.

Data availability All the data are presented within the article or in the supplementary material.

Declarations

Ethics approval This project was approved by the Academic Commission of ethics, of the Biological and Health Sciences Division, Universidad Autónoma Metropolitana, Unidad Iztapapa, with the number 1851.

Consent to participate All the authors of this work voluntarily consented to participate in it.

Consent for publication All the authors of this work consented to its publication.

Conflict of interest The authors declare that they have no conflict of interest.

References

- López-Otín C, Blasco MA, Partridge L, Serrano M, Kroemer G. The hallmarks of aging. *Cell*. 2013;153(6):1194–217.
- Organization WH. World report on ageing and health: World Health Organization; 2015.
- Austad SN, Fischer KE. Sex differences in lifespan. *Cell Metab*. 2016;23(6):1022–33.
- Miller RA, Harrison DE, Astle CM, Fernandez E, Flurkey K, Han M, et al. Rapamycin-mediated lifespan increase in mice is dose and sex dependent and metabolically distinct from dietary restriction. *Aging Cell*. 2014;13(3):468–77.
- Austad SN. Sex differences in health and aging: a dialog between the brain and gonad? *GeroScience*. 2019:1–7.
- Choleris E, Galea LA, Sohrabji F, Frick KM. Sex differences in the brain: Implications for behavioral and biomedical research. *Neurosci Biobehav Rev*. 2018;85:126–45.
- Hernandez AR, Truckenbrod LM, Campos KT, Williams SA, Burke SN. Sex differences in age-related impairments vary across cognitive and physical assessments in rats. *Behav Neurosci*. 2019.
- Luine V, Gomez J, Beck K, Bowman R. Sex differences in chronic stress effects on cognition in rodents. *Pharmacol Biochem Behav*. 2017;152:13–9.
- Friedman J. Why is the nervous system vulnerable to oxidative stress? Oxidative stress and free radical damage in neurology: Springer; 2011. p. 19–27.
- Pérez-Severiano F, Salvatierra-Sánchez R, Rodríguez-Pérez M, Cuevas-Martínez EY, Guevara J, Limón D, et al. S-Allylcysteine prevents amyloid- β peptide-induced oxidative stress in rat hippocampus and ameliorates learning deficits. *Eur J Pharmacol*. 2004;489(3):197–202.
- Colin-Gonzalez A, Aguilera G, N Serratos I, M Escribano B, Santamaria A, Tunes I. On the relationship between the light/dark cycle, melatonin and oxidative stress. *Curr Pharm Des*. 2015;21(24):3477–88.
- Ibáñez-Contreras A, Hernández-Arciga U, Poblano A, Arteaga-Silva M, Hernández-Godínez B, Mendoza-Cuevas G, et al. Electrical activity of sensory pathways in female and male geriatric Rhesus monkeys (*Macaca mulatta*), and its relation to oxidative stress. *Exp Gerontol*. 2018;101:80–94.
- Torrens-Mas M, Pons D-G, Sastre-Serra J, Oliver J, Roca P. Sexual hormones regulate the redox status and mitochondrial function in the brain. Pathological implications. *Redox Biol*. 2020;101505.
- Pérez VI, Bokov A, Van Remmen H, Mele J, Ran Q, Ikeno Y, et al. Is the oxidative stress theory of aging dead? *Biochim Biophys Acta (BBA) - Gen Subj*. 2009;1790(10):1005–14.
- Sims-Robinson C, Hur J, Hayes JM, Dauch JR, Keller PJ, Brooks SV, et al. The role of oxidative stress in nervous system aging. *PLoS One*. 2013;8(7):e68011.
- Chang L, Munsaka SM, Kraft-Terry S, Ernst T. Magnetic resonance spectroscopy to assess neuroinflammation and neuropathic pain. *J NeuroImmune Pharmacol*. 2013;8(3):576–93.
- Warburton EC, Brown MW. Findings from animals concerning when interactions between perirhinal cortex, hippocampus and medial prefrontal cortex are necessary for recognition memory. *Neuropsychologia*. 2010;48(8):2262–72.
- Annavarapu RN, Kathi S, Vadla VK. Non-invasive imaging modalities to study neurodegenerative diseases of aging brain. *J Chem Neuroanat*. 2019;95:54–69.

19. Bassar PJ, Mattiello J, LeBihan D. Estimation of the effective self-diffusion tensor from the NMR spin echo. *J Magn Reson Ser B*. 1994;103(3):247–54.
20. Sullivan EV, Pfefferbaum A. Diffusion tensor imaging and aging. *Neurosci Biobehav Rev*. 2006;30(6):749–61.
21. Duarte JM, Do KQ, Gruetter R. Longitudinal neurochemical modifications in the aging mouse brain measured in vivo by 1H magnetic resonance spectroscopy. *Neurobiol Aging*. 2014;35(7):1660–8.
22. Paoletti F, Aldinucci D, Mocali A, Caparrini A. A sensitive spectrophotometric method for the determination of superoxide dismutase activity in tissue extracts. *Anal Biochem*. 1986;154(2):536–41.
23. Hernández-Arciga U, Herrera MLG, Ibáñez-Contreras A, Miranda-Labra RU, Flores-Martínez JJ, Königsberg M. Baseline and post-stress seasonal changes in immunocompetence and redox state maintenance in the fishing bat *Myotis vivesi*. *PLoS One*. 2018;13(1):e0190047.
24. Aebi H. [13] Catalase in vitro. *Methods in enzymology*: Elsevier; 1984. p. 121–6.
25. Hernández-Arciga U, Hernández-Álvarez D, López-Cervantes SP, López-Díazguerrero NE, Alarcón-Aguilar A, Luna-López A, et al. Effect of long-term moderate-exercise combined with metformin-treatment on antioxidant enzymes activity and expression in the gastrocnemius of old female Wistar rats. *Biogerontology*. 2020:1–19.
26. Hernández-Álvarez D, Mena-Montes B, Toledo-Pérez R, Pedraza-Vázquez G, López-Cervantes SP, Morales-Salazar A, et al. Long-term moderate exercise combined with metformin treatment induces an hormetic response that prevents strength and muscle mass loss in old female wistar rats. *Oxidative Med Cell Longev*. 2019;2019:1–14.
27. Gámiz F, Gallo M. Spontaneous object recognition memory in aged rats: Complexity versus similarity. *Learn Mem*. 2012;19(10):444–8.
28. Schneider CA, Rasband WS, Eliceiri KW. NIH Image to ImageJ: 25 years of image analysis. *Nat Methods*. 2012;9(7):671–5.
29. Tournier J-D, Smith R, Raffelt D, Tabbara R, Dhollander T, Pietsch M, et al. MRtrix3: A fast, flexible and open software framework for medical image processing and visualisation. *NeuroImage*. 2019;202:116137.
30. Heiland S, Sartor K, Martin E, Bardenheuer HJ, Plaschke K. In vivo monitoring of age-related changes in rat brain using quantitative diffusion magnetic resonance imaging and magnetic resonance relaxometry. *Neurosci Lett*. 2002;334(3):157–60.
31. Zárate S, Stevnsner T, Gredilla R. Role of estrogen and other sex hormones in brain aging. *Neuroprotection and DNA repair*. *Front Aging Neurosci*. 2017;9:430.
32. Pluvinage JV, Wyss-Coray T. Systemic factors as mediators of brain homeostasis, ageing and neurodegeneration. *Nat Rev Neurosci*. 2020:1–10.
33. Harraan D. Aging: a theory based on free radical and radiation chemistry. 1955.
34. Jones DP. Redox theory of aging. *Redox Biol*. 2015;5:71–9.
35. Kunath S, Moosmann B. What is the rate-limiting step towards aging? Chemical reaction kinetics might reconcile contradictory observations in experimental aging research. *GeroScience*. 2019:1–10.
36. Calabrese V, Butterfield D, Stella A. Aging and oxidative stress response in the CNS. *Development and Aging Chang Nerv Syst Handb Neurochem Mol Neurobiol*. 2008;3:128–234.
37. Franco R, Vargas MR. Redox biology in neurological function, dysfunction, and aging. New Rochelle: Mary Ann Liebert, Inc.; 2018.
38. Webb W, Adler RK. *Neurology for the Speech-Language Pathologist-E-Book*: Elsevier health sciences; 2016.
39. Ezzyat Y, Olson IR. The medial temporal lobe and visual working memory: comparisons across tasks, delays, and visual similarity. *Cogn Affect Behav Neurosci*. 2008;8(1):32–40.
40. Dröge W, Schipper HM. Oxidative stress and aberrant signaling in aging and cognitive decline. *Aging Cell*. 2007;6(3):361–70.
41. Schuessel K, Leutner S, Cairns N, Müller W, Eckert A. Impact of gender on upregulation of antioxidant defence mechanisms in Alzheimer's disease brain. *J Neural Transm*. 2004;111(9):1167–82.
42. Malorni W, Campesi I, Straface E, Vella S, Franconi F. Redox features of the cell: a gender perspective. *Antioxid Redox Signal*. 2007;9(11):1779–802.
43. Khalifa ARM, Abdel-Rahman EA, Mahmoud AM, Ali MH, Noureldin M, Saber SH, et al. Sex-specific differences in mitochondria biogenesis, morphology, respiratory function, and ROS homeostasis in young mouse heart and brain. *Phys Rep*. 2017;5(6):e13125.
44. Ruszkiewicz JA, Miranda-Vizuete A, Tinkov AA, Skalnaya MG, Skalny AV, Tsatsakis A, et al. Sex-specific differences in redox homeostasis in brain norm and disease. *J Mol Neurosci*. 2019;67(2):312–42.
45. Irwin RW, Yao J, Hamilton RT, Cadenas E, Brinton RD, Nilsen J. Progesterone and estrogen regulate oxidative metabolism in brain mitochondria. *Endocrinology*. 2008;149(6):3167–75.
46. Guevara R, Gianotti M, Oliver J, Roca P. Age and sex-related changes in rat brain mitochondrial oxidative status. *Exp Gerontol*. 2011;46(11):923–8.
47. Stebbings KA, Choi HW, Ravindra A, Llano DA. The impact of aging, hearing loss, and body weight on mouse hippocampal redox state, measured in brain slices using fluorescence imaging. *Neurobiol Aging*. 2016;42:101–9.
48. Casado Á, López-Fernández ME, Casado MC, de La Torre R. Lipid peroxidation and antioxidant enzyme activities in vascular and Alzheimer dementias. *Neurochem Res*. 2008;33(3):450–8.
49. Wang L, Ahn YJ, Asmis R. Sexual dimorphism in glutathione metabolism and glutathione-dependent responses. *Redox Biol*. 2020;31:101410.
50. Alves Oliveira AC, Dionizio A, Teixeira FB, Bittencourt LO, Nonato Miranda GH, Oliveira Lopes G, et al. Hippocampal Impairment Triggered by Long-Term Lead Exposure from Adolescence to Adulthood in Rats: Insights from Molecular to Functional Levels. *Int J Mol Sci*. 2020;21(18):6937.
51. Gakhar M, Verma S, Lehri A. A comparison of nerve conduction properties in male and female of 20 to 30 years of age group. *J Exerc Sci Physiother*. 2014;10(1):16.

52. Kumari SK, Kannan U, Patil AB. Influence of age, height, gender on median and ulnar nerve conduction study. *Natl J Physiol Pharm Pharmacol*. 2018;8(2):202–6.
53. Reed TE, Vernon PA, Johnson AM. Sex difference in brain nerve conduction velocity in normal humans. *Neuropsychologia*. 2004;42(12):1709–14.
54. Sharma R, Joshi S, Singh K, Kumar A. Visual evoked potentials: normative values and gender differences. *J Clin Diagn Res*. 2015;9(7):CC12–5.
55. Gupta S, Mittal S, Baweja P, Kumar A, Singh KD, Sharma R. Analysis of gender based differences in auditory evoked potentials among healthy elderly population. *Adv Biomed Res*. 2014;3:208.
56. Krizman J, Skoe E, Kraus N. Sex differences in auditory subcortical function. *Clin Neurophysiol*. 2012;123(3):590–7.
57. Walsh ME, Sloane LB, Fischer KE, Austad SN, Richardson A, Van Remmen H. Use of nerve conduction velocity to assess peripheral nerve health in aging mice. *J Gerontol Ser A: Biomed Sci Med Sci*. 2015;70(11):1312–9.
58. Fontanesi LB, Fazan FS, Dias FJ, Schiavoni MCL, Marques W Jr, Fazan VPS. Sensory and motor conduction velocity in spontaneously hypertensive rats: sex and aging investigation. *Front Syst Neurosci*. 2019;13.
59. Kuba M, Kubová Z, Kremláček J, Langrová J. Motion-onset VEPs: characteristics, methods, and diagnostic use. *Vis Res*. 2007;47(2):189–202.
60. Ravera S, Bartolucci M, Cuccarolo P, Litamè E, Illario M, Calzia D, et al. Oxidative stress in myelin sheath: The other face of the extramitochondrial oxidative phosphorylation ability. *Free Radic Res*. 2015;49(9):1156–64.
61. Ibáñez-Contreras A, Poblano A, Arteaga-Silva M, Hernández-Godínez B, Hernández-Arciga U, Toledo R, et al. Visual, auditive and somatosensory pathways alterations in geriatric rhesus monkeys (*Macaca mulatta*). *J Med Primatol*. 2016;45(2):92–102.
62. Verdú E, Ceballos D, Vilches JJ, Navarro X. Influence of aging on peripheral nerve function and regeneration. *J Peripher Nerv Syst*. 2000;5(4):191–208.
63. Haynes RL, Folkert RD, Szweda LI, Volpe JJ, Kinney HC. Lipid peroxidation during human cerebral myelination. *J Neuropathol Exp Neurol*. 2006;65(9):894–904.
64. Stahon KE, Bastian C, Griffith S, Kidd GJ, Brunet S, Baltan S. Age-related changes in axonal and mitochondrial ultrastructure and function in white matter. *J Neurosci*. 2016;36(39):9990–10001.
65. Patel R, Sesti F. Oxidation of ion channels in the aging nervous system. *Brain Res*. 1639;2016:174–85.
66. Morrison CD, Pistell PJ, Ingram DK, Johnson WD, Liu Y, Fernandez-Kim SO, et al. High fat diet increases hippocampal oxidative stress and cognitive impairment in aged mice: implications for decreased Nrf2 signaling. *J Neurochem*. 2010;114(6):1581–9.
67. Iguchi Y, Kosugi S, Nishikawa H, Lin Z, Minabe Y, Toda S. Repeated exposure of adult rats to transient oxidative stress induces various long-lasting alterations in cognitive and behavioral functions. *PLoS One*. 2014;9(12):e114024.
68. Treviño S, Aguilar-Alonso P, Flores Hernandez JA, Brambila E, Guevara J, Flores G, et al. A high calorie diet causes memory loss, metabolic syndrome and oxidative stress into hippocampus and temporal cortex of rats. *Synapse*. 2015;69(9):421–33.
69. Logan S, Royce GH, Owen D, Farley J, Ranjo-Bishop M, Sonntag WE, et al. Accelerated decline in cognition in a mouse model of increased oxidative stress. *GeroScience*. 2019;41(5):591–607.
70. Concha L. A macroscopic view of microstructure: using diffusion-weighted images to infer damage, repair, and plasticity of white matter. *Neuroscience*. 2014;276:14–28.
71. Fleysler R, Lipton ML, Noskin O, Rundek T, Lipton R, Derby CA. White matter structural integrity and transcranial Doppler blood flow pulsatility in normal aging. *Magn Reson Imaging*. 2018;47:97–102.
72. Anderova M, Vorisek I, Pivonkova H, Benesova J, Vargova L, Cicanic M, et al. Cell death/proliferation and alterations in glial morphology contribute to changes in diffusivity in the rat hippocampus after hypoxia—ischemia. *J Cereb Blood Flow Metab*. 2011;31(3):894–907.
73. Syková E, Mazel T, Šimonová Z. Diffusion constraints and neuron–glia interaction during aging. *Exp Gerontol*. 1998;33(7-8):837–51.
74. Syková E, Nicholson C. Diffusion in brain extracellular space. *Physiol Rev*. 2008;88(4):1277–340.
75. Vargová L, Syková E. Astrocytes and extracellular matrix in extrasynaptic volume transmission. *Philos Trans R Soc B: Biol Sci*. 2014;369(1654):20130608.
76. Jones DK, Basser PJ. “Squashing peanuts and smashing pumpkins”: how noise distorts diffusion-weighted MR data. *Magnet Reson Med*. 2004;52(5):979–93.
77. Merelli A, Repetto M, Lazarowski A, Auzmendi J. Hypoxia, Oxidative Stress, and Inflammation: Three Faces of Neurodegenerative Diseases. *J Alzheimers Dis*. 2020(Preprint):1–18.
78. Engelter ST, Provenzale JM, Petrella JR, DeLong DM, MacFall JR. The effect of aging on the apparent diffusion coefficient of normal-appearing white matter. *Am J Roentgenol*. 2000;175(2):425–30.
79. Cámara E, Bodammer N, Rodríguez-Fornells A, Tempelmann C. Age-related water diffusion changes in human brain: a voxel-based approach. *Neuroimage*. 2007;34(4):1588–99.
80. Walhovd KB, Fjell AM, Reinvang I, Lundervold A, Dale AM, Eilertsen DE, et al. Effects of age on volumes of cortex, white matter and subcortical structures. *Neurobiol Aging*. 2005;26(9):1261–70.
81. Hamezah HS, Durani LW, Ibrahim NF, Yanagisawa D, Kato T, Shiino A, et al. Volumetric changes in the aging rat brain and its impact on cognitive and locomotor functions. *Exp Gerontol*. 2017;99:69–79.
82. Giorgio A, Santelli L, Tomassini V, Bosnell R, Smith S, De Stefano N, et al. Age-related changes in grey and white matter structure throughout adulthood. *Neuroimage*. 2010;51(3):943–51.
83. Moffett JR, Ross B, Arun P, Madhavarao CN, Namboodiri AM. N-Acetylaspartate in the CNS: from neurodiagnostics to neurobiology. *Prog Neurobiol*. 2007;81(2):89–131.
84. Harris JL, Choi I-Y, Brooks WM. Probing astrocyte metabolism in vivo: proton magnetic resonance spectroscopy in the injured and aging brain. *Front Aging Neurosci*. 2015;7:202.

85. Benarroch EE. N-acetylaspartate and N-acetylaspartylglutamate: neurobiology and clinical significance. *Neurology*. 2008;70(16):1353–7.
86. Brand A, Richter-Landsberg C, Leibfritz D. Multinuclear NMR studies on the energy metabolism of glial and neuronal cells. *Dev Neurosci*. 1993;15(3-5):289–98.
87. Bitsch A, Bruhn H, Vougioukas V, Stringaris A, Lassmann H, Frahm J, et al. Inflammatory CNS demyelination: histopathologic correlation with in vivo quantitative proton MR spectroscopy. *Am J Neuroradiol*. 1999;20(9):1619–27.
88. Reyngoudt H, Claeys T, Vlerick L, Verleden S, Acou M, Deblaere K, et al. Age-related differences in metabolites in the posterior cingulate cortex and hippocampus of normal ageing brain: a 1H-MRS study. *Eur J Radiol*. 2012;81(3):e223–e31.
89. Gemmati D, Bramanti B, Serino ML, Secchiero P, Zauli G, Tisato V. COVID-19 and Individual Genetic Susceptibility/Receptivity: Role of ACE1/ACE2 Genes, Immunity, Inflammation and Coagulation. Might the Double X-Chromosome in Females Be Protective against SARS-CoV-2 Compared to the Single X-Chromosome in Males? *Int J Mol Sci*. 2020;21(10):3474.
90. Ongun N, Oguzhanoglu A. Comparison of the nerve conduction parameters in proximally and distally located muscles innervated by the bundles of median and ulnar nerves. *Med Princ Pract*. 2016;25(5):466–71.

Publisher's note Springer Nature remains neutral with regard to jurisdictional claims in published maps and institutional affiliations.